

## Computer modelling of divalent, trivalent and tetravalent ion doping in $\text{LiCaAlF}_6$ and $\text{LiSrAlF}_6$

This article has been downloaded from IOPscience. Please scroll down to see the full text article.

2004 J. Phys.: Condens. Matter 16 8733

(<http://iopscience.iop.org/0953-8984/16/47/023>)

View [the table of contents for this issue](#), or go to the [journal homepage](#) for more

Download details:

IP Address: 129.252.86.83

The article was downloaded on 27/05/2010 at 19:13

Please note that [terms and conditions apply](#).

# Computer modelling of divalent, trivalent and tetravalent ion doping in $\text{LiCaAlF}_6$ and $\text{LiSrAlF}_6$

J B Amaral<sup>1</sup>, A C Lewis<sup>2</sup>, M E G Valerio<sup>1,3</sup> and R A Jackson<sup>2,3</sup>

<sup>1</sup> Departamento de Física, Universidade Federal de Sergipe, 49.100-000 São Cristovão-SE, Brazil

<sup>2</sup> Lennard-Jones Laboratories, School of Chemistry and Physics, Keele University, Keele, Staffordshire ST5 5BG, UK

E-mail: mvalerio@fisica.ufs.br and r.a.jackson@chem.keele.ac.uk

Received 12 May 2004, in final form 2 November 2004

Published 12 November 2004

Online at [stacks.iop.org/JPhysCM/16/8733](http://stacks.iop.org/JPhysCM/16/8733)

doi:10.1088/0953-8984/16/47/023

## Abstract

This paper describes a computational study of the mixed metal fluorides  $\text{LiCaAlF}_6$  and  $\text{LiSrAlF}_6$ , doped with divalent ( $\text{Pb}^{2+}$ ,  $\text{Co}^{2+}$  and  $\text{Ni}^{2+}$ ), trivalent ( $\text{Cr}^{3+}$ ,  $\text{Fe}^{3+}$  and  $\text{Y}^{3+}$ ) and tetravalent ( $\text{Si}^{4+}$ ) ions. For each of the frameworks, all three cation sites were considered, as well as a range of charge compensation mechanisms. For the divalent dopants, substitution at the divalent host site is preferred, whilst for the trivalent dopants,  $\text{Co}^{3+}$  and  $\text{Fe}^{3+}$  prefer the  $\text{Al}^{3+}$  site, and  $\text{Y}^{3+}$  shows behaviour similar to the rare earths. Finally, it is found that  $\text{Al}^{3+}$  is the preferred site for substitution by  $\text{Si}^{4+}$  in both host frameworks.

## 1. Introduction

The mixed metal fluorides  $\text{LiCaAlF}_6$  and  $\text{LiSrAlF}_6$  are being investigated for use in photonic devices because they are good hosts for optically active cations and can be grown easily [1]. When doped with rare earth ions, these materials show useful optical properties, as demonstrated in a range of publications [2–5]. Computer modelling has been used in a recent study of rare earth doping in these materials [6] and in addition, the crystal field parameters have been obtained, enabling predictions of the optical activity to be made [7].

In this paper, doping of  $\text{LiCaAlF}_6$  and  $\text{LiSrAlF}_6$  by a range of divalent, trivalent and tetravalent ions is considered. It is noted that divalent ion doping produces laser properties in other fluoride materials, for example the doping of  $\text{BaLiF}_3$  by  $\text{Pb}^{2+}$ ,  $\text{Ni}^{2+}$  and  $\text{Co}^{2+}$ . In particular, the absorption spectroscopic properties of the transition metal ions  $\text{Ni}^{2+}$  and  $\text{Co}^{2+}$  and the de-excitation mechanisms of  $\text{Ni}^{2+}$  in  $\text{BaLiF}_3$  have been reported recently [8–12]. Due to their vibronic emission characteristics, the materials, when doped with these ions, are potentially tunable laser active media over a range of hundreds of nanometres in the 1500 nm

<sup>3</sup> Authors to whom any correspondence should be addressed.

**Table 1.** Interatomic potentials for LiCaAlF<sub>6</sub> and LiSrAlF<sub>6</sub>.

Interaction	A (eV)	$\rho$ (Å)	C (eV Å <sup>6</sup> )	k (eV Å <sup>-2</sup> )
(a) LiCaAlF <sub>6</sub> /LiSrAlF <sub>6</sub> framework potentials				
Li <sup>+</sup> core F <sup>-</sup> shell	443.83	0.2714	0.0	—
Al <sup>3+</sup> core F <sup>-</sup> shell	1400.00	0.2571	0.0	—
Ca <sup>2+</sup> core F <sup>-</sup> shell	3400.00	0.2661	0.0	—
Sr <sup>2+</sup> core F <sup>-</sup> shell	3400.00	0.2906	0.0	—
F <sup>-</sup> shell F <sup>-</sup> shell	911.69	0.2707	13.80	—
F <sup>-</sup> core F <sup>-</sup> shell	—	—	—	24.36
(b) Dopant–framework potentials				
Pb <sup>2+</sup> core F <sup>-</sup> shell	400.0	0.4115	0.0	—
Co <sup>2+</sup> core F <sup>-</sup> shell	1613.5	0.2668	0.0	—
Ni <sup>2+</sup> core F <sup>-</sup> shell	1599.7	0.2626	0.0	—
Cr <sup>3+</sup> core F <sup>-</sup> shell	949.7	0.2895	0.0	—
Fe <sup>3+</sup> core F <sup>-</sup> shell	1993.0	0.2620	0.0	—
Y <sup>3+</sup> core F <sup>-</sup> shell	1650.0	0.3020	0.0	—
Si <sup>4+</sup> core F <sup>-</sup> shell	1773.4	0.2571	0.0	—

spectral region, which is important in telecommunications applications. Apart from BaLiF<sub>3</sub>, laser characteristics have been reported in a range of crystal hosts with Co<sup>2+</sup> and Ni<sup>2+</sup> ions as dopants [13–17].

In Pb<sup>2+</sup> doped BaLiF<sub>3</sub>, colour centres were created by high-energy electron irradiation, generating Pb<sup>+</sup> centres. These have been investigated as potential candidates for laser active media [18].

Apart from the rare earth ions, doping LiCaAlF<sub>6</sub> and LiSrAlF<sub>6</sub> by other trivalent ions can be important. For example, Cr<sup>3+</sup> doped LiCaAlF<sub>6</sub> and LiSrAlF<sub>6</sub> have been extensively studied and currently they are being used as TW solid-state laser media [19–21]. Also, in some natural materials, Fe<sup>3+</sup> gives rise to colour centres.

In addition to these dopants, Y<sup>3+</sup> has been included in the study because it has similar chemical properties to the rare earth ions, and it was not included in [6], and Si<sup>4+</sup> has been considered as a representative tetravalent dopant ion.

## 2. Computational method

The methodology adopted in this paper follows the procedure adopted in the previous paper on intrinsic defects and rare earth ion doping in LiCaAlF<sub>6</sub> and LiSrAlF<sub>6</sub> [6]. A brief summary of the important points of procedure now follows.

### 2.1. Derivation of potentials

The derivation of potentials for the LiCaAlF<sub>6</sub> and LiSrAlF<sub>6</sub> frameworks has been described in [6]; the potentials themselves are given in table 1. The potentials for the dopant–framework interactions were obtained as described in the following subsections.

**2.1.1. Divalent dopants.** The dopant ions considered were Pb<sup>2+</sup>, Co<sup>2+</sup> and Ni<sup>2+</sup>, and potentials to describe their interactions with the frameworks were taken from an earlier study of divalent dopants in BaLiF<sub>3</sub> where their derivation is described [22]. The potentials are given in table 1.

**Table 2.** Lattice energies.

Material	$E_{\text{latt}}$ (eV)
LiF	-10.93
CaF <sub>2</sub>	-26.99
SrF <sub>2</sub>	-24.47
AlF <sub>3</sub>	-63.99
PbF <sub>2</sub>	-22.35
CoF <sub>2</sub>	-28.64
NiF <sub>2</sub>	-29.29
YF <sub>3</sub>	-52.17
CrF <sub>3</sub>	-60.10
FeF <sub>3</sub>	-59.41
SiF <sub>4</sub>	-102.65

*2.1.2. Trivalent dopants.* The potentials describing the interaction between trivalent dopants and the frameworks were obtained by fitting to the CrF<sub>3</sub>, FeF<sub>3</sub> and YF<sub>3</sub> structures. The potentials are given in table 1.

*2.1.3. Tetravalent dopants.* The potential to describe the Si<sup>4+</sup>-F<sup>-</sup> interaction was taken from a previous paper [23]. It was fitted to the F-topaz structure, and tested by calculating the SiF<sub>4</sub> structure and comparing with experimental lattice parameters. It is given in table 1.

## 2.2. Defect calculations

Calculations of defects and of ion doping were performed using the Mott–Littleton method [24] in which atoms in a spherical region immediately surrounding the defect are treated explicitly, and a continuum approach is used for more distant regions of the lattice. This method has been used widely and successfully in modelling defects in ionic solids.

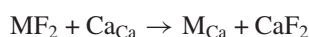
In calculating the energetics of doping, the substitution energy is first calculated. This quantity cannot be used for comparison purposes, and instead the solution energy is calculated, which is defined as the total energy involved in the doping process, including charge compensation if needed. The calculation of solution energies, and the different reaction schemes involved in ion doping, are discussed in section 3.

## 3. Results

### 3.1. Divalent doping

The dopants considered in this work are Pb<sup>2+</sup>, Co<sup>2+</sup> and Ni<sup>2+</sup>. They can substitute at any of the three possible cation sites in the framework materials. The substitution energies are given in table 3.

If they substitute at the Ca<sup>2+</sup> or Sr<sup>2+</sup> site, no charge compensation is needed. The solution energies are calculated using the following reaction (using LiCaAlF<sub>6</sub> as an example):



where M is a divalent dopant, and Kroger–Vink notation has been used.

Based on this reaction, the solution energy is obtained from the expression below:

$$E_{\text{sol}} = -E_{\text{latt}}(\text{MF}_2) + E_{\text{subs}}(\text{M}_{\text{Ca}}) + E_{\text{latt}}(\text{CaF}_2).$$

**Table 3.** Substitution energies (eV).

Dopant	LiSrAlF <sub>6</sub>			LiCaAlF <sub>6</sub>		
	M <sub>Li</sub>	M <sub>Sr</sub>	M <sub>Al</sub>	M <sub>Li</sub>	M <sub>Ca</sub>	M <sub>Al</sub>
Divalent						
Co <sup>2+</sup>	-13.4	-3.5	32.4	-12.9	-2.02	32.5
Ni <sup>2+</sup>	-14.0	-3.8	31.8	-13.6	-2.37	31.8
Pb <sup>2+</sup>	-4.0	2.1	41.6	-3.1	4.84	42.2
Trivalent						
Cr <sup>3+</sup>	-37.59	-28.62	4.31	-36.86	-26.93	4.34
Fe <sup>3+</sup>	-36.79	-28.32	5.25	-36.06	-26.57	5.31
Y <sup>3+</sup>	-28.60	-22.38	13.83	-27.80	-20.25	14.05
Tetravalent						
Si <sup>4+</sup>	-74.55	-67.40	-36.35	-73.45	-65.17	-35.96

In this expression the lattice energies are assumed to take negative values, and are given in table 2.

Alternatively, substitution at either the Li<sup>+</sup> or Al<sup>3+</sup> sites will require charge compensation. If substitution takes place at the Li<sup>+</sup> site, compensation by the formation of Li<sup>+</sup> vacancies has been assumed, as in the following reaction:

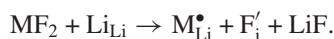


The solution energy is then as follows:

$$E_{\text{sol}} = -E_{\text{latt}}(\text{MF}_2) + E_{\text{subs}}(\text{M}_{\text{Li}}^{\bullet}) + E(\text{V}_{\text{Li}}') + 2E_{\text{latt}}(\text{LiF}).$$

Charge compensation by F<sup>-</sup> interstitials has not been considered because in all cases the calculated solution energies are higher.

The reaction involved is:



This then gives the following expression for the solution energy:

$$E_{\text{sol}} = -E_{\text{latt}}(\text{MF}_2) + E_{\text{subs}}(\text{M}_{\text{Li}}^{\bullet}) + E(\text{F}_{\text{i}}') + E_{\text{latt}}(\text{LiF}).$$

For example, considering Co<sup>2+</sup> substitution at the Li<sup>+</sup> site in LiCaAlF<sub>6</sub>, the unbound solution energy is 2.79 eV, as opposed to 1.90 eV for V<sub>Li</sub>' compensation.

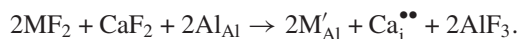
For substitution at the Al<sup>3+</sup> site, F<sup>-</sup> vacancy compensation has been assumed, as in the reaction below:



The solution energy is then given by:

$$E_{\text{sol}} = -E_{\text{latt}}(\text{MF}_2) + E_{\text{subs}}(\text{M}_{\text{Al}}') + E(\text{V}_{\text{F}}^{\bullet}) + E_{\text{latt}}(\text{AlF}_3).$$

Charge compensation by cation interstitials has not been considered because it leads to higher solution energies. A reaction scheme involving Ca<sup>2+</sup> interstitials is given below:



The solution energy with this scheme would be given by:

$$E_{\text{sol}} = -2E_{\text{latt}}(\text{MF}_2) - E_{\text{latt}}(\text{CaF}_2) + 2E_{\text{subs}}(\text{M}_{\text{Al}}') + E(\text{Ca}_{\text{i}}^{\bullet\bullet}) + 2E_{\text{latt}}(\text{AlF}_3).$$

**Table 4.** (a) Unbound and (b) bound divalent dopant solution energies (eV).

Defect	LiSrAlF <sub>6</sub>			LiCaAlF <sub>6</sub>		
	Co <sup>2+</sup>	Ni <sup>2+</sup>	Pb <sup>2+</sup>	Co <sup>2+</sup>	Ni <sup>2+</sup>	Pb <sup>2+</sup>
(a)						
M <sub>Li</sub> <sup>•</sup> -V <sub>Li</sub> '	1.90	1.94	5.01	2.20	2.15	5.71
M <sub>Ca/Sr</sub>	<b>0.67</b>	<b>1.02</b>	<b>-0.02</b>	<b>-0.37</b>	<b>-0.07</b>	<b>0.20</b>
M <sub>Al</sub> '-V <sub>F</sub> <sup>•</sup>	9.03	9.18	17.76	10.62	10.47	20.85
(b)						
M <sub>Li</sub> <sup>•</sup> -V <sub>Li</sub> '	1.20	1.24	4.20	1.34	1.37	4.54
M <sub>Ca/Sr</sub>	<b>0.67</b>	<b>1.02</b>	<b>-0.02</b>	<b>-0.37</b>	<b>-0.07</b>	<b>0.20</b>
M <sub>Al</sub> '-V <sub>F</sub> <sup>•</sup>	2.46	2.51	3.94	1.75	1.74	5.30

Considering Co<sup>2+</sup> substitution in LiSrAlF<sub>6</sub> using this scheme, the unbound solution energy is 18.70 eV, as opposed to 9.03 eV for F<sup>-</sup> vacancy compensation.

In all of the above expressions, values for the vacancy energies  $E(V'_{Li})$  and  $E(V^{\bullet}_{F})$  are taken from [6]. The solution energies are reported in tables 4(a) and (b). The energies reported in table 4(a) have been calculated assuming that there is no interaction between the dopant and the charge-compensating defect. This implies that the energies quoted are for unbound defects. On the other hand, in table 4(b), the calculations were carried out for a configuration consisting of the dopant and charge-compensating defects in neighbouring positions, meaning that the energies include the contribution of the binding energy of the defect.

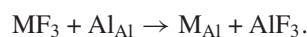
It is seen that there is an energetic preference for incorporation of dopants at the divalent site for both frameworks, although both Ni<sup>2+</sup> and Co<sup>2+</sup> also have low solution energies at the Li<sup>+</sup> site, assuming charge compensation by Li<sup>+</sup> vacancies. This result may appear intuitively obvious, but in the case of BaLiF<sub>3</sub> [22], it was found that solution at the monovalent site is preferred for Co<sup>2+</sup> and Ni<sup>2+</sup>, while Pb<sup>2+</sup> prefers the divalent site. The explanation for this difference in behaviour is that ion size is the key issue in BaLiF<sub>3</sub>, while in LiCaAlF<sub>6</sub> and LiSrAlF<sub>6</sub> the charge compensation energy would appear to be the dominating factor.

Finally, it is seen that there is a larger change in solution energy in going from unbound to bound defect configurations for the substitution at the Al<sup>3+</sup> site with F<sup>-</sup> vacancy compensation than that observed for the other cases. This can be explained by the much higher binding energy due to the increased electrostatic interaction between the defect species in this case, which is in turn due to their being in nearest neighbour positions.

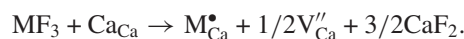
### 3.2. Trivalent doping

Cr<sup>3+</sup>, Y<sup>3+</sup> and Fe<sup>3+</sup> doping has been considered in this section. The ions can substitute at any of the cation sites, with charge compensation required at the Ca<sup>2+</sup>/Sr<sup>2+</sup> and Li<sup>+</sup> sites. The substitution schemes and accompanying reactions are given below:

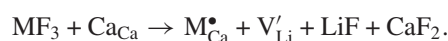
- (i) M<sup>3+</sup> at Al<sup>3+</sup> (no charge compensation)



- (ii) M<sup>3+</sup> at Ca<sup>2+</sup>/Sr<sup>2+</sup>, with charge compensation by Ca<sup>2+</sup>/Sr<sup>2+</sup> vacancies



- (iii) M<sup>3+</sup> at Ca<sup>2+</sup>/Sr<sup>2+</sup>, with charge compensation by Li<sup>+</sup> vacancies



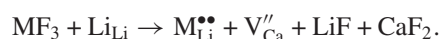
- (iv)  $M^{3+}$  at  $Ca^{2+}/Sr^{2+}$ , with charge compensation by  $F^-$  interstitials (3 interstitial sites considered)



- (v)  $M^{3+}$  at  $Li^+$ , with charge compensation by  $Li^+$  vacancies



- (vi)  $M^{3+}$  at  $Li^+$ , with charge compensation by  $Ca^{2+}/Sr^{2+}$  vacancies



- (vii)  $M^{3+}$  at  $Li^+$ , with charge compensation by  $F^-$  interstitials (three interstitial sites considered)



As in the case of the divalent dopants, the solution energies for each of the above schemes were calculated for either unbound or bound defects, and the results are given in tables 5(a) and (b) respectively. For the interstitial  $F^-$  ions, the same sites were used in these calculations as in the previous paper on rare earth doping [6].

In table 5(b), it is seen that there are differences in behaviour both between the dopant ions and the host frameworks. In both frameworks,  $Cr^{3+}$  and  $Fe^{3+}$  will be incorporated at the  $Al^{3+}$  site, since the solution energies are lower. Conversely, the behaviour of  $Y^{3+}$  depends on the framework; for  $LiSrAlF_6$ , incorporation at the  $Sr^{2+}$  site with  $F^-$  interstitial compensation is clearly preferred, but for  $LiCaAlF_6$ , there are two possibilities, (i) incorporation at the  $Ca^{2+}$  site with  $Li^+$  vacancy compensation, and (ii) incorporation at the  $Li^+$  site with  $Ca^{2+}$  vacancy compensation.

In the previous paper [6], it was found that when doping  $LiCaAlF_6$  with one of the rare earth ions within the series from Pr to Tm, both substitution at the  $Ca^{2+}$  site with  $Li^+$  vacancy compensation and substitution at the  $Li^+$  site with  $Ca^{2+}$  vacancy compensation gave very similar energies, a trend also observed here when doping  $LiCaAlF_6$  with  $Y^{3+}$ . It seems that the dominating effect in the case of  $LiCaAlF_6$  is the ionic size of the dopant, and  $Y^{3+}$  just fits in the rare earth series from Pr to Tm with an ionic radius very similar to that of Ho.

In the case of the  $LiSrAlF_6$  framework, the previous work indicates that the rare earth series is divided into two sections. From La to Ho, substitution at the  $Sr^{2+}$  site with  $F^-$  interstitial compensation is favoured, and from Er to Lu, substitution at the  $Al^{3+}$  site is preferred. Since the ionic radius of  $Y^{3+}$  is 90 pm [25], just below the  $Ho^{3+}$  radius (90.1 pm), it is expected that it should behave like the rare earth ions in the first group, consistent with the results obtained in the present work.

The other two dopants,  $Cr^{3+}$  and  $Fe^{3+}$ , on the other hand are very small, compared to the rare earth ions or to  $Y^{3+}$ . The  $Fe^{3+}$  size is 64.5 pm, while the  $Cr^{3+}$  size is 61.5 pm, closer to the size of the  $Al^{3+}$  ion (53.5 pm). This explains why, in both frameworks,  $Cr^{3+}$  and  $Fe^{3+}$  will preferentially substitute at the  $Al^{3+}$  site.

Without the binding contribution (table 5(a)), the preferred site would be  $Al^{3+}$  for all three dopants in both frameworks. For  $Y^{3+}$ , when binding is taken into account, the behaviour changes completely. In some cases, like  $Y_{Li}^{\bullet\bullet}-V_{Ca}''$  in  $LiCaAlF_6$ , the binding energy (defined as the difference between the energy of formation of bound and unbound defect complexes) is as large as  $-8.54$  eV, decreasing the solution energy to 1.51 eV. This can be understood since both interacting isolated defects have equal and opposite charges, and the Coulombic energy can be high enough to make this defect one of the most energetically favourable. Similar behaviour is observed for both Cr and Fe, but in these cases the magnitude of the binding contribution is not enough to change the trend, i.e., the incorporation of these two dopants at the  $Al^{3+}$  site.

**Table 5.** (a) Unbound and (b) bound trivalent solution energies (per dopant) (eV). ‘NC’ means calculation did not converge.

Defect	LiSrAlF <sub>6</sub>			LiCaAlF <sub>6</sub>		
	Cr <sup>3+</sup>	Fe <sup>3+</sup>	Y <sup>3+</sup>	Cr <sup>3+</sup>	Fe <sup>3+</sup>	Y <sup>3+</sup>
(a)						
M <sub>Al</sub>	<b>0.42</b>	<b>0.67</b>	<b>2.01</b>	<b>0.45</b>	<b>0.73</b>	<b>2.23</b>
M <sub>Ca/Sr</sub> <sup>•</sup> - $\frac{1}{2}$ V <sub>Ca/Sr</sub> <sup>''</sup>	5.24	4.85	3.56	4.28	3.95	3.03
M <sub>Ca/Sr</sub> <sup>•</sup> -V <sub>Li</sub> <sup>'</sup>	4.59	4.21	2.91	3.57	3.23	2.32
M <sub>Ca/Sr</sub> <sup>•</sup> -F <sub>i</sub> <sup>'</sup> F <sub>i</sub> <sup>'</sup> at ( $\frac{1}{4}$ $\frac{1}{4}$ 0)	4.64	4.26	2.96	3.80	3.46	2.55
M <sub>Ca/Sr</sub> <sup>•</sup> -F <sub>i</sub> <sup>'</sup> F <sub>i</sub> <sup>'</sup> at ( $\frac{1}{2}$ $\frac{1}{2}$ 0)	5.08	4.70	3.40	4.16	3.82	2.91
M <sub>Ca/Sr</sub> <sup>•</sup> -F <sub>i</sub> <sup>'</sup> F <sub>i</sub> <sup>'</sup> at ( $\frac{3}{4}$ $\frac{1}{2}$ 0)	4.54	4.16	2.86	4.16	3.82	2.91
M <sub>Li</sub> <sup>••</sup> -2V <sub>Li</sub> <sup>'</sup>	6.76	6.87	7.82	7.09	7.20	8.22
M <sub>Li</sub> <sup>••</sup> -V <sub>Ca/Sr</sub> <sup>''</sup>	8.05	8.16	9.11	8.52	8.63	9.65
M <sub>Li</sub> <sup>••</sup> -2F <sub>i</sub> <sup>'</sup> F <sub>i</sub> <sup>'</sup> at ( $\frac{1}{4}$ $\frac{1}{4}$ 0), ( $\frac{1}{2}$ $\frac{1}{2}$ 0)	7.30	7.41	8.36	7.91	8.02	9.04
M <sub>Li</sub> <sup>••</sup> -2F <sub>i</sub> <sup>'</sup> F <sub>i</sub> <sup>'</sup> at ( $\frac{1}{4}$ $\frac{1}{4}$ 0), ( $\frac{3}{4}$ $\frac{1}{2}$ 0)	6.76	6.87	7.82	7.91	8.02	9.04
M <sub>Li</sub> <sup>••</sup> -2F <sub>i</sub> <sup>'</sup> F <sub>i</sub> <sup>'</sup> at ( $\frac{1}{2}$ $\frac{1}{2}$ 0), ( $\frac{3}{4}$ $\frac{1}{2}$ 0)	7.20	7.31	8.26	8.27	8.38	9.40
(b)						
M <sub>Al</sub>	<b>0.42</b>	<b>0.67</b>	2.01	<b>0.45</b>	<b>0.73</b>	2.23
M <sub>Ca/Sr</sub> <sup>•</sup> - $\frac{1}{2}$ V <sub>Ca/Sr</sub> <sup>''</sup>	4.54	4.13	2.74	NC	3.08	2.01
M <sub>Ca/Sr</sub> <sup>•</sup> -V <sub>Li</sub> <sup>'</sup>	4.04	11.26	2.25	2.79	2.46	<b>1.50</b>
M <sub>Ca/Sr</sub> <sup>•</sup> -F <sub>i</sub> <sup>'</sup> F <sub>i</sub> <sup>'</sup> at ( $\frac{1}{4}$ $\frac{1}{4}$ 0)	3.81	3.35	<b>1.76</b>	3.33	2.69	1.57
M <sub>Ca/Sr</sub> <sup>•</sup> -F <sub>i</sub> <sup>'</sup> F <sub>i</sub> <sup>'</sup> at ( $\frac{1}{2}$ $\frac{1}{2}$ 0)	3.86	3.35	<b>1.76</b>	3.19	2.66	NC
M <sub>Ca/Sr</sub> <sup>•</sup> -F <sub>i</sub> <sup>'</sup> F <sub>i</sub> <sup>'</sup> at ( $\frac{3}{4}$ $\frac{1}{2}$ 0)	3.92	3.35	<b>1.76</b>	3.13	2.66	1.70
M <sub>Li</sub> <sup>••</sup> -2V <sub>Li</sub> <sup>'</sup>	4.70	4.77	5.45	4.76	4.89	4.25
M <sub>Li</sub> <sup>••</sup> -V <sub>Ca/Sr</sub> <sup>''</sup>	4.54	4.13	2.74	5.45	5.53	<b>1.51</b>
M <sub>Li</sub> <sup>••</sup> -2F <sub>i</sub> <sup>'</sup> F <sub>i</sub> <sup>'</sup> at ( $\frac{1}{4}$ $\frac{1}{4}$ 0), ( $\frac{1}{2}$ $\frac{1}{2}$ 0)	15.97	NC	3.17	3.22	5.70	4.29
M <sub>Li</sub> <sup>••</sup> -2F <sub>i</sub> <sup>'</sup> F <sub>i</sub> <sup>'</sup> at ( $\frac{1}{4}$ $\frac{1}{4}$ 0), ( $\frac{3}{4}$ $\frac{1}{2}$ 0)	NC	NC	2.51	3.30	NC	4.77
M <sub>Li</sub> <sup>••</sup> -2F <sub>i</sub> <sup>'</sup> F <sub>i</sub> <sup>'</sup> at ( $\frac{1}{2}$ $\frac{1}{2}$ 0), ( $\frac{3}{4}$ $\frac{1}{2}$ 0)	NC	NC	3.83	3.23	3.72	NC

In two cases, it is seen that the bound solution energies are higher than the unbound values; this is the case for Cr<sub>Li</sub><sup>••</sup>-2F<sub>i</sub><sup>'</sup> and for Fe<sub>Sr</sub><sup>•</sup>-V<sub>Li</sub><sup>'</sup> in the LiSrAlF<sub>6</sub> framework. A careful analysis of the relaxed configurations revealed large distortions in the surrounding lattice. As a consequence of this, the amount of energy gained in the binding process is insufficient to compensate the energy resulting from the distortion, meaning that, in these two cases, the defects are likely to be unbound. Also, in a few other cases, the calculations of bound defects did not converge (as indicated by ‘NC’ in the tables); this was caused by a high degree of distortion in the defect configurations, which would not be expected to be stable.

Finally, it is noted that all the solution energies are positive. However, the values for Cr<sup>3+</sup> and Fe<sup>3+</sup> are low. This explains why it is possible to make samples containing relatively large amounts of Cr<sup>3+</sup>, while suggesting the potential difficulty of producing samples containing, for example, Y<sup>3+</sup>.

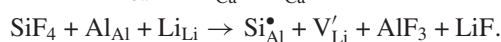
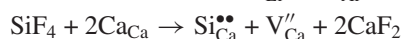


**Table 6.** Si<sup>4+</sup> tetravalent defect solution energies (eV). ‘NC’ means calculation did not converge.

Defect	LiSrAlF <sub>6</sub>	LiCaAlF <sub>6</sub>
Unbound		
Si <sub>Li</sub> <sup>••••</sup> -V <sub>Al</sub> <sup>'''</sup>	10.98	14.01
Si <sub>Ca/Sr</sub> <sup>••</sup> -V <sub>Ca</sub> <sup>''</sup>	6.05	5.50
Si <sub>Al</sub> <sup>•</sup> -V <sub>Li</sub> <sup>'</sup>	<b>1.30</b>	<b>-1.11</b>
Bound		
Si <sub>Li</sub> <sup>••••</sup> -V <sub>Al</sub> <sup>'''</sup>	2.82	NC
Si <sub>Ca/Sr</sub> <sup>••</sup> -V <sub>Ca/Sr</sub> <sup>''</sup>	7.2	NC
Si <sub>Al</sub> <sup>•</sup> -V <sub>Li</sub> <sup>'</sup>	<b>-0.82</b>	<b>-1.05</b>

### 3.3. Tetravalent doping

As an example of tetravalent doping, Si<sup>4+</sup> has been considered. In this case, charge compensation is needed for substitution at all three cation sites. The three reaction schemes are given below for the case of LiCaAlF<sub>6</sub>:



The first reaction represents the incorporation of Si<sup>4+</sup> at the Li<sup>+</sup> site being compensated by formation of Al<sup>3+</sup> vacancies. The second reaction describes the substitution of the Si<sup>4+</sup> ion at the Ca<sup>2+</sup> site with charge compensation via Ca<sup>2+</sup> vacancies. The last one describes substitution at the Al<sup>3+</sup> site, with compensation by Li<sup>+</sup> vacancies.

As in the last two subsections, unbound and bound solution energies have been calculated, and these are reported in table 6. It is quite clear that the preferred mode of substitution is at the Al<sup>3+</sup> site, with charge compensation by Li<sup>+</sup> vacancies. This would be expected since the Si<sup>4+</sup> and Al<sup>3+</sup> ions have similar ionic radii.

## 4. Conclusions

The paper has presented a study of defect structure and doping in LiCaAlF<sub>6</sub> and LiSrAlF<sub>6</sub> by a range of divalent, trivalent and tetravalent ions. The predicted sites for doping have been calculated and rationalized on the basis of the structural differences between the two materials, and can be summarized as follows:

- Co<sup>2+</sup>, Ni<sup>2+</sup> and Pb<sup>2+</sup> substitute at the Ca<sup>2+</sup> or Sr<sup>2+</sup> site as appropriate.
- Cr<sup>3+</sup> and Fe<sup>3+</sup> substitute at the Al<sup>3+</sup> site in both frameworks.
- Y<sup>3+</sup> in LiSrAlF<sub>6</sub> substitutes at the Sr<sup>2+</sup> site with F<sup>-</sup> interstitial compensation.
- Y<sup>3+</sup> in LiCaAlF<sub>6</sub> substitutes either at the Ca<sup>2+</sup> site with Li<sup>+</sup> vacancy compensation or at the Li<sup>+</sup> site with Ca<sup>2+</sup> vacancy compensation.
- Si<sup>4+</sup> substitutes at the Al<sup>3+</sup> site in both frameworks with Li<sup>+</sup> vacancy compensation.

This information is of use when doped LiCaAlF<sub>6</sub> or LiSrAlF<sub>6</sub> are used in device applications, where the first step to understanding the optical behaviour of the doped material requires the dopant site to be known. This procedure is further discussed in a recent paper on the optical behaviour of rare earth doped LiCaAlF<sub>6</sub>/LiSrAlF<sub>6</sub> [26]; the calculations in the

present paper will enable this procedure to be extended to the other dopant ions considered here.

Finally, the paper builds on the conclusions of the previous study [6], which was concerned with rare earth doping in these materials, and helps to provide a fully comprehensive picture of ion doping in LiCaAlF<sub>6</sub> and LiSrAlF<sub>6</sub>.

### Acknowledgments

The authors are grateful to CNPq and CAPES for financial support. JBA acknowledges the award of a studentship grant from PIBIC/CNPq-UFS.

### References

- [1] Hughes D W and Barr J R M 1992 *J. Phys. D: Appl. Phys.* **25** 563
- [2] Sarantopoulou E, Kollia Z and Cefalas A C 2000 *Microelectron. Eng.* **53** 105
- [3] Liu Z, Kozeki T, Suzuki Y and Sarukura N 2001 *Opt. Lett.* **26** 301
- [4] Dubinskii M A, Semashko V V, Naumov A K, Abdulsabirov R Y and Korableva S L 1993 *Laser Phys.* **3** 216
- [5] Marshall C D, Payne S A, Speth J A, Krupke W F, Quarles G J, Castillo V and Chai B H T 1994 *J. Opt. Soc. Am. B* **11** 2054
- [6] Amaral J B, Plant D F, Valerio M E G and Jackson R A 2003 *J. Phys.: Condens. Matter* **15** 2523
- [7] Amaral J B, Valerio M E G, Couto dos Santos M A and Jackson R A 2004 *Nucl. Instrum. Methods Phys. Res. B* **218C** 232
- [8] Martins E, Vieira N D Jr, Baldochi S L, Morato S P and Gesland J Y 1994 *J. Lumin.* **62** 281
- [9] Baldochi S L, Santo A M E, Martins E, Duarte M, Vieira M M F, Vieira N D Jr and Morato S P 1996 *J. Cryst. Growth* **166** 375
- [10] Duarte M, Martins E, Baldochi S L, Morato S P, Vieira N D Jr and Vieira M M F 1998 *Opt. Commun.* **151** 366
- [11] Duarte M, Martins E, Baldochi S L, Vieira N D Jr and Vieira M M F 1999 *Opt. Commun.* **159** 221
- [12] Martins E, Duarte M, Baldochi S L, Morato S P, Vieira M M F and Vieira N D Jr 1997 *J. Phys. Chem. Solids* **58** 655
- [13] Iverson M V and Sibley W A 1979 *J. Lumin.* **20** 311
- [14] Mollenauer L F and White J C 1987 *Top. Appl. Phys.* **59** 1
- [15] Penzkofer A 1988 *Prog. Quantum Electron.* **12** 291
- [16] Moulton P F 1982 *IEEE J. Quantum Electron.* **18** 1185
- [17] Villacampa B, Cases R, Orera V M and Alcalá R 1994 *J. Phys. Chem. Solids* **55** 263
- [18] Prado L, Vieira N D Jr, Baldochi S L, Morato S P, Denis J P, Tercier N and Blanzat B 1996 *J. Phys. Chem. Solids* **57** 413
- [19] Zhang W, Wang C-Y, Zhao J, Chai L and Xing Q 1998 *Opt. Laser Technol.* **30** 551
- [20] Fromzel V A and Prasad C R 2001 *J. Phys. Chem. Solids* **62** 865
- [21] Parsons-Karavassilis D, Gu Y, Ansari Z, French P M W and Taylor J R 2000 *Opt. Commun.* **181** 361
- [22] Valerio M E G, Jackson R A and de Lima J F 1998 *J. Phys.: Condens. Matter* **10** 3353
- [23] Jackson R A and Valerio M E G 2004 *J. Phys.: Condens. Matter* **16** S2771
- [24] Mott N F and Littleton M J 1938 *Trans. Faraday Soc.* **34** 485
- [25] Shannon R D 1976 *Acta Crystallogr. A* **32** 751
- [26] Jackson R A, Valerio M E G, Couto dos Santos M A and Amaral J B 2004 *Dalton Trans.* **19** 3098